

# A Novel Multiparameter *In Vitro* Model of Three-Dimensional Cell Ingress Into Scaffolds for Dermal Reconstruction to Predict *In Vivo* Outcome

Elena García-Gareta, Nivedita Ravindran, Vaibhav Sharma, Sorousheh Samizadeh, and Julian F. Dye

## Abstract

The clinical demand for effective dermal substitutes continues as current commercially available products present limitations. However, there are no definitive *in vitro* methods to predict *in vivo* outcomes such as integration, cellularization and contraction, which may help the development of new dermal scaffolds. This study aimed to develop a multiparameter *in vitro* model of three-dimensional (3D) cell ingress into dermal scaffolds to predict *in vivo* outcomes of new dermal scaffolds under development. A new dermal scaffold, Smart Matrix, was compared to the scar-forming contractile collagen gel model and to the clinically well-established Integra<sup>®</sup> and Matriderm<sup>®</sup>. Parameters studied were cell viability and proliferation, apoptosis, matrix contraction, cell morphology,  $\alpha$ -smooth muscle actin, and growth factor expression. Combinatorial evaluation of the results in a scoring matrix showed that Smart Matrix could offer an advantage over existing products. This method would be useful as an international golden scoring matrix to develop new dermal scaffolds that effectively improve the existing products, thus enabling better treatments for burns or chronic wounds.

**Key words:** biomaterials; tissue engineering; wounds

## Introduction

**D**ERMAL SUBSTITUTES FOR TREATING burns or chronic wounds, which have risen worldwide due to an increment in life expectancy and developments in intensive care, are some of the first examples of tissue engineering. They are made of natural biological materials (Alloderm<sup>®</sup>, Lifecell Corp., Branchburg, NJ), natural (Integra<sup>®</sup>, Integra LifeSciences, Plainsboro, NJ; Matriderm<sup>®</sup>, Skin & Health Care AG, Billerbeck, Germany) or artificial (Polyactive<sup>®</sup>, Octopus NV, Leider, The Netherlands) polymers and some of them include cells (Dermagraft<sup>®</sup>, Smith & Nephew, Hull, United Kingdom). They protect the wound from infection and fluid loss and allow the attachment and ingrowth of cells that will form new dermis rather than scar tissue. However, limitations of current products include unreliable integration, poor mechanical properties, size limitations, or high costs. Thus, the clinical need for dermal substitutes continues to be high.<sup>5-7</sup>

Developing new dermal scaffolds requires *in vitro* testing before *in vivo* experimentation in animal models and ultimately clinical trials. There are many examples in the literature of *in vitro* testing of new scaffolds for dermal

reconstruction, which focus on mechanical characterization of the biomaterial, cytotoxicity, and investigation of certain cell-matrix interactions relevant to wound healing.<sup>8-14</sup> However, there are no studies attempting to standardize *in vitro* testing of new dermal scaffolds, which could predict *in vivo* outcomes such as integration, cellularization, and contraction.

Several critical cellular factors may be proposed that contribute to the overall *in vivo* healing trajectory, such as cell viability and proliferation, apoptosis, matrix contraction, alpha-smooth muscle actin ( $\alpha$ -SMA), and growth factors expression. These parameters may also allow responses to different scaffolds to be identified. The objectives of this study were (1) to develop a multiparameter *in vitro* model of three-dimensional (3D) cell ingress into dermal scaffolds that studies the main events of wound healing and (2) to evaluate the results in a combinatory manner with a scoring matrix to predict *in vivo* outcome, thus establishing the necessity for further *in vivo* testing of the new dermal scaffold under development. The overall aim of the study was to establish this method as the international golden standard scoring matrix for *in vitro* evaluation of new dermal scaffolds.

---

RAFT Institute of Plastic Surgery, Mount Vernon Hospital, Northwood, United Kingdom.

This article was previously published in abstract form at the 2013 annual meetings of TERMIS EU (Abstract no. 665),<sup>1</sup> the Tissue and Cell Engineering Society (proceedings published in *European Cells and Materials*),<sup>2</sup> and the European Tissue Repair Society (proceedings published in *Wound Repair and Regeneration*).<sup>3</sup> A poster version of this article has been published online by the RAFT Institute.<sup>4</sup>

## Materials and Methods

### Cell culture

Primary human dermal fibroblasts (HDFs) from three donors were established from routine surgical excisions of normal skin, obtained with informed consent and local ethics committee approval. Pieces of dissected skin (1 mm × 1 mm) were cultured dermal side down in T25 tissue culture flasks (eight per flask), in 3 mL of Dulbecco's modified Eagle's medium (DMEM, 31885-023, Gibco, Paisley, United Kingdom) supplemented with 10% fetal calf serum (10270-106, Gibco), 100 U/mL penicillin and streptomycin (15140-122, Gibco), and 100  $\mu$ M L-glutamine (25030-024, Gibco) at 37°C with 5% CO<sub>2</sub>. Medium was changed twice per week. Adherent HDF egress cultures typically establish within 3 weeks. Cells were used at passage 4.

### Control monolayer cultures

HDFs ( $5 \times 10^5$ ) in 50  $\mu$ L were seeded on 13-mm-diameter borosilicate glass coverslips (631-0150, VWR International, Leighton Buzzard, United Kingdom) in 12-well plates. After 30-min incubation at 37°C with 5% CO<sub>2</sub>, 2 mL of supplemented DMEM was added per well and plates cultured at 37°C with 5% CO<sub>2</sub>. Medium was changed every 3 days.

### 3D-contractile collagen gels

Collagen type I from rat tail tendons, 2.1 mg/mL in 0.6% acetic acid (60-30-810, First Link Ltd, Wolverhampton, United Kingdom), was supplemented with 10X 199 medium (M0650, Sigma-Aldrich, Gillingham, United Kingdom), and approximately 2% (v/v) of 7.5% NaHCO<sub>3</sub>, buffered with 1.4% (v/v) 1 M HEPES pH 7.4; pH was neutralized by adding 1 M NaOH dropwise, assessed by color change from yellow to scarlet. Reagents were kept in an ice bath during preparation as well as the final collagen mixture until mixed with the cells.<sup>15,16</sup> Cells ( $5 \times 10^5$ ) were mixed with 0.5 mL of collagen mixture, plated into 24-well plates and allowed to polymerize within 60 min at 37°C with 5% CO<sub>2</sub>. Two milliliters of supplemented DMEM were added per well. Gels were gently freed from the plastic surface and allowed to float in the culture medium. Medium was changed every 3 days.

### Dermal scaffolds

The following dermal scaffolds were used: (1) Integra, 2.1-mm-thick bilayer of bovine tendon collagen type I/chondroitin-6-sulfate crosslinked with glutaraldehyde and a silicon backing; (2) Matrigel, 1-mm-thick lyophilized layer of bovine collagen types I, III, and V/elasticity; and (3) Smart Matrix, 2-mm-thick freeze-dried sheet of bovine fibrin/alginate crosslinked with glutaraldehyde, manufactured in our laboratory.

Dermal scaffolds were cut into 6-mm-diameter discs and tightly fitted in a 96-well plate. Cells ( $5 \times 10^5$ ) in 50  $\mu$ L were seeded per scaffold. Two hundred microliters of supplemented DMEM were added per well, and plates were cultured overnight at 37°C with 5% CO<sub>2</sub>. Scaffolds were transferred to 24-well plates and supplemented with 2 mL of culture medium. Medium was changed every 3 days.

### Cell viability and proliferation by alamarBlue activity assay

One milliliter of 10% alamarBlue (DAL1025, Invitrogen™, Paisley, United Kingdom) stock diluted into phenol-free sup-

plemented DMEM (11880, Gibco) was added per well and incubated at 37°C with 5% CO<sub>2</sub> for 3 h. For each sample, 1 mL was transferred to a cuvette (FB55147, Fisher Scientific, Loughborough, United Kingdom), and following the manufacturer's instructions, absorbance was measured at 570 nm against air using a M550 double beam UV/visible spectrophotometer (Spectronic Camspec Ltd., Garforth, United Kingdom). Absorbance at 600 nm of phenol-free DMEM was subtracted from sample values.

### Annexin V apoptosis assay

TACS Annexin V-Biotin kit (4835-01-K, Trevigen, Abingdon, United Kingdom) was used. Annexin V-Biotin working reagent was 1  $\mu$ L of Annexin V-Biotin, 10  $\mu$ L of 10× binding buffer and 89  $\mu$ L of distilled water, diluted 1/100 in phosphate-buffered saline (PBS) and stored in the dark on ice. Samples were washed with cold PBS, incubated in 100  $\mu$ L Annexin V-Biotin working reagent for 15 min in the dark at room temperature, washed with 1× binding buffer, incubated with 100  $\mu$ L of streptavidin-fluorescein isothiocyanate (F0422, Dako, Glostrup, Denmark; 1:200 in 1× binding buffer) in the dark at room temperature for 15 min, washed twice with 1× binding buffer and fixed in 4% paraformaldehyde overnight. Samples were washed twice with PBS, permeabilized with two drops of 0.5% Triton X-100/PBS for 5 min at room temperature, washed three times with PBS, and incubated in block buffer (0.5% bovine serum albumin [BSA]/PBS, pH 7.4) for 30 min at room temperature. Block buffer was drained into tissue paper and samples were incubated in Alexa Fluor 546-phalloidin (A22283, Invitrogen, Carlsbad, CA; 1:100 in block buffer), for 1 h at room temperature inside a dark humidified chamber, washed five times in wash buffer (0.1% Triton X-100/0.1% BSA/PBS, pH 7.4), then once in PBS and once in distilled water. Samples were transferred to slides with one drop of Vecta Mount™ (H-5000, Vector, Peterborough, United Kingdom) and viewed under a confocal laser microscope (Leica DMIRE2, Leica Microsystems GmbH, Wetzlar, Germany).

### Ki67 and $\alpha$ -SMA expression

At days 2 and 7 of culture, specimens were fixed in 4% paraformaldehyde overnight and processed as already described in a previous section with Ki67 (Mouse Anti-Rat Ki-67 Antigen, M7248, Dako; 1:100 in block buffer) or  $\alpha$ -SMA (Mouse Monoclonal Anti-Actin  $\alpha$ -Smooth Muscle, A2547, Sigma-Aldrich; 1:1000 in block buffer) as primary antibodies. Secondary antibody (Alexa Fluor 546, goat anti-mouse, A11003, Invitrogen, USA; 1:100 in block buffer) was used with green phalloidin for Ki67 immunostained samples (Alexa Fluor 488 phalloidin, A12379, Invitrogen, USA; 1:100 in block buffer). Samples were examined by confocal microscopy.

### Scanning electron microscopy

Fixed specimens (2.5% glutaraldehyde, Agar Scientific, Stansted, United Kingdom) were washed with 0.1 M sodium cacodylate buffer (Agar Scientific) and postfixed in 1% osmium tetroxide (Sigma-Aldrich) in cacodylate buffer for 1 h; then washed in cacodylate buffer, dehydrated through a graded series of industrial methylated spirit (20%–60%) and ethanol (70%–100%), equilibrated in 100% ethanol and left to dry overnight. Specimens were mounted on stubs, gold sputtered coated (Agar Auto Sputter Coater, Agar Scientific)

and observed (FEI Inspect F, Oxford Instruments, Oxford, United Kingdom).

### Histology

Fixed specimens (4% paraformaldehyde) were embedded in paraffin. Four-micrometer sections were taken for hematoxylin and eosin staining and viewed under light microscopy (Zeiss Axiophot, Zeiss, Jena, Germany) with a DC200 Leica digital camera and IC50 software.

### Cytokine/growth factor expression profile

On days 2 and 7 of culture expression of tumor necrosis factor alpha (TNF $\alpha$ ), insulin-like growth factor 1 (IGF1), vascular endothelial growth factor (VEGF), interleukin (IL)-6, fibroblast growth factor b (bFGF), transforming growth factor beta (TGF $\beta$ ), epidermal growth factor (EGF), and leptin was profiled (EA-1011, Signosis Inc., Sunnyvale, CA). Supernatants (100  $\mu$ L/well) were pipetted into coated wells and incubated for 1 h at room temperature with gentle shaking, after which wells were washed three times with 200  $\mu$ L of wash buffer. Diluted biotin-labeled antibody mixture (100  $\mu$ L/well) was added and incubated as before. After repeating the washing step, diluted streptavidin-horseradish peroxidase conjugate (100  $\mu$ L/well) was added and incubated for 45 min at room temperature with gentle shaking. After washing, substrate (100  $\mu$ L/well) was added, followed after 30-min incubation by stop solution (50  $\mu$ L/well). Absorbance at 450 nm was measured using a microplate reader (Biorad 550, Biorad, Hemel Hempstead, United Kingdom).

### Statistical analysis

Comparisons between groups were made using one-way analysis of variance (SigmaStat 3.5 software). A  $p$ -value  $\leq 0.05$  was considered a significant result.

### Scoring matrix

Combinatorial evaluation of results was done with a scoring matrix: (1) the new dermal scaffold under evaluation, Smart Matrix, was compared to contractile collagen gels (CCGs), established model of scar formation,<sup>9</sup> and to the clinically well-established Integra and Matriderm;<sup>17-21</sup> (2) no difference between Smart Matrix and the scaffold of reference was marked with 0, a positive difference with 1, and a negative difference with -1. A total positive score suggests an improvement over existing products and therefore the new scaffold should be further evaluated *in vivo*. A negative score or 0 suggests no improvement, and therefore no further *in vivo* evaluation is recommended.

## Results

### SEM of dermal scaffolds

The three dermal scaffolds used present microporosity (Fig. 1). In addition, Matriderm and Smart Matrix have nanofibers, densely packed in Smart Matrix, as well as nanopores.

### Matrix contraction

The three dermal scaffolds did not contract, while CCGs contracted down to 20% of the initial area (Fig. 1).

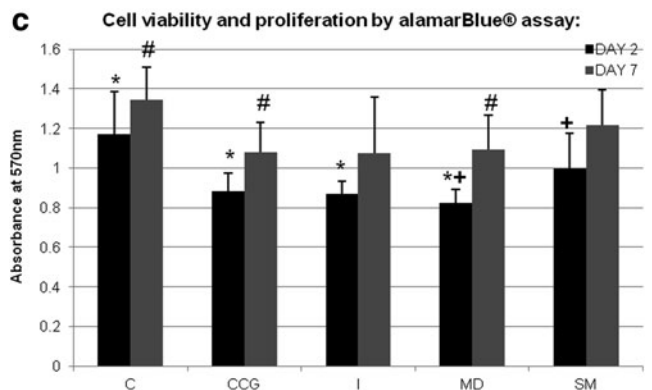
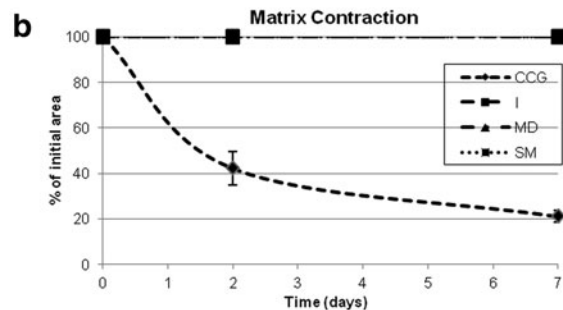
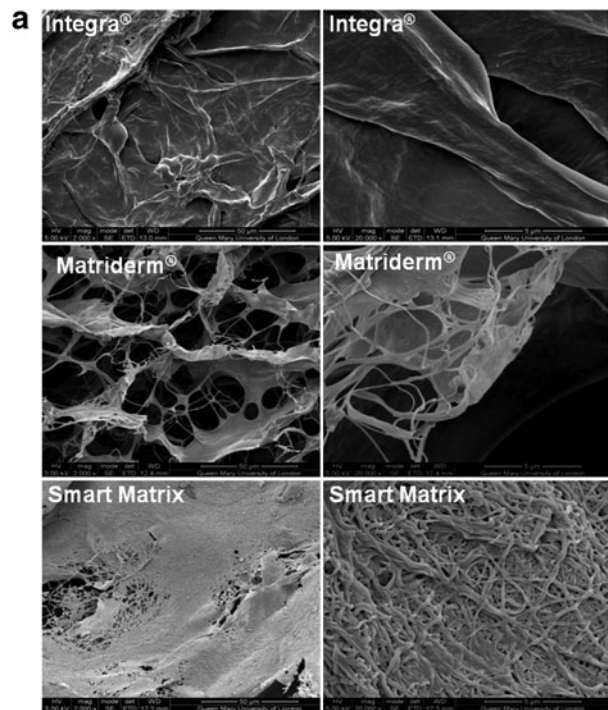


**FIG. 1.** (a) Scanning electron microscopy (SEM) photos of dermal scaffolds. (b) Matrix contraction of contractile collagen gels (CCG), Integra (I), Matriderm (MD), and Smart Matrix (SM). (c) Cell viability and proliferation by alamarBlue assay of monolayer control (C), contractile collagen gels (CCG), Integra (I), Matriderm (MD) and Smart Matrix (SM) at days 2 and 7 of culture (\*C at day 2 significantly higher,  $p < 0.05$ , than CCG, I, and MD; #C at day 7 significantly higher,  $p < 0.05$ , than CCG and MD; +SM at day 2 significantly higher,  $p < 0.05$ , than MD; significant increase in alamarBlue activity,  $p < 0.05$ , between days 2 and 7 for C, CCG, MD, and SM).

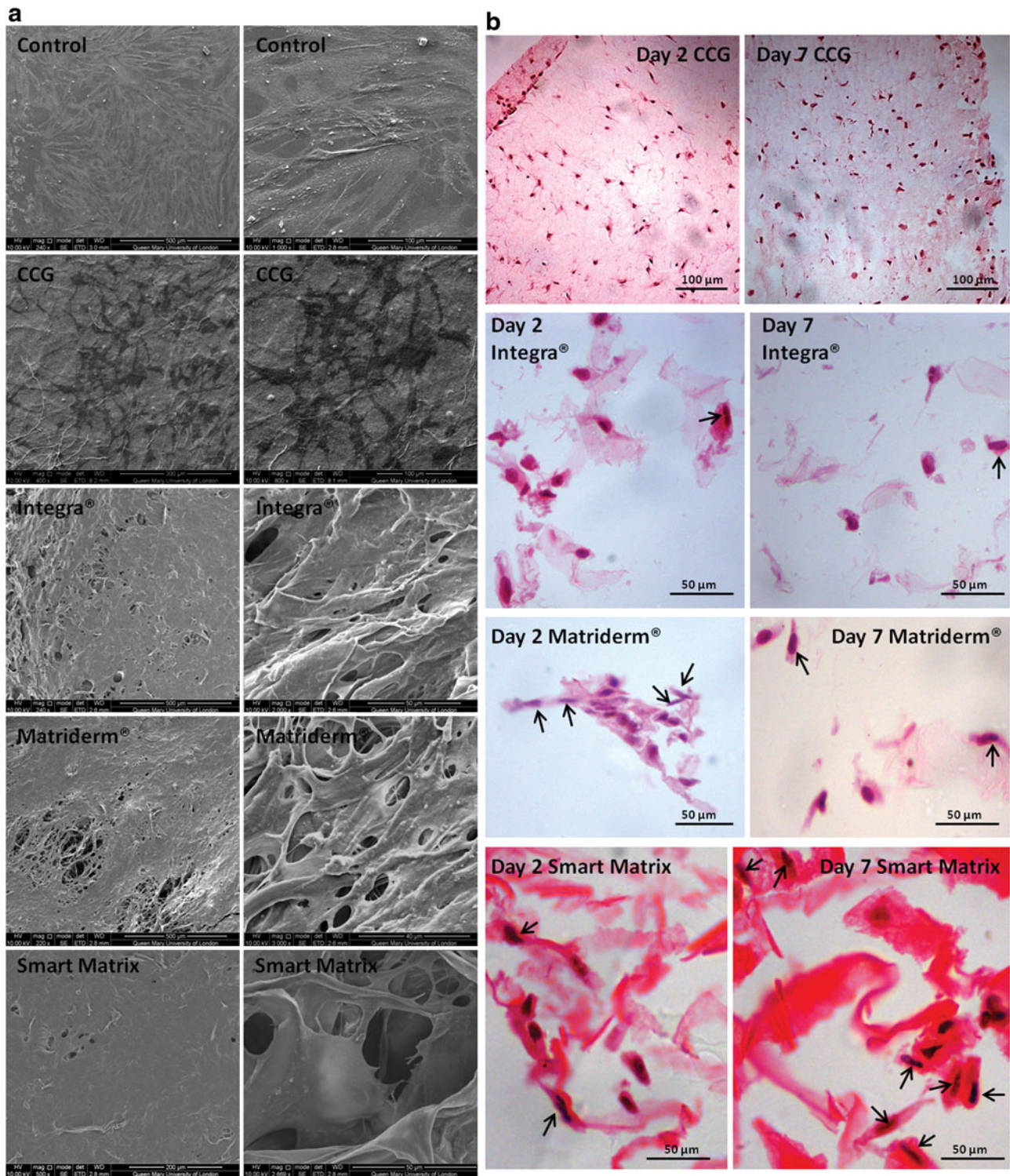


**FIG. 2.** (a) SEM photos of monolayer control (day 2), contractile collagen gel (day 7), Integra (day 2), Matrigel (day 2), and Smart Matrix (day 2) cultured with normal human dermal fibroblasts. (b) Hematoxylin and eosin (H&E) staining of 4- $\mu$ m cross-sections of the different matrices cultured with normal human dermal fibroblasts for 2 and 7 days. Black arrows point at cells with elongated morphology.

#### Cell proliferation and viability

AlamarBlue activity, a colorimetric redox assay of metabolic activity and thus of cell viability and proliferation,<sup>22</sup> significantly ( $p < 0.05$ ) increased between days 2

and 7 for all samples and controls except for Integra (Fig. 1). Monolayer cultures showed statistically significant higher activities compared to CCGs ( $p = 0.002$ ), Integra ( $p = 0.001$ ) and Matrigel ( $p < 0.001$ ) at day 2, and CCGs ( $p = 0.009$ ) and Matrigel ( $p = 0.047$ ) at day 7.

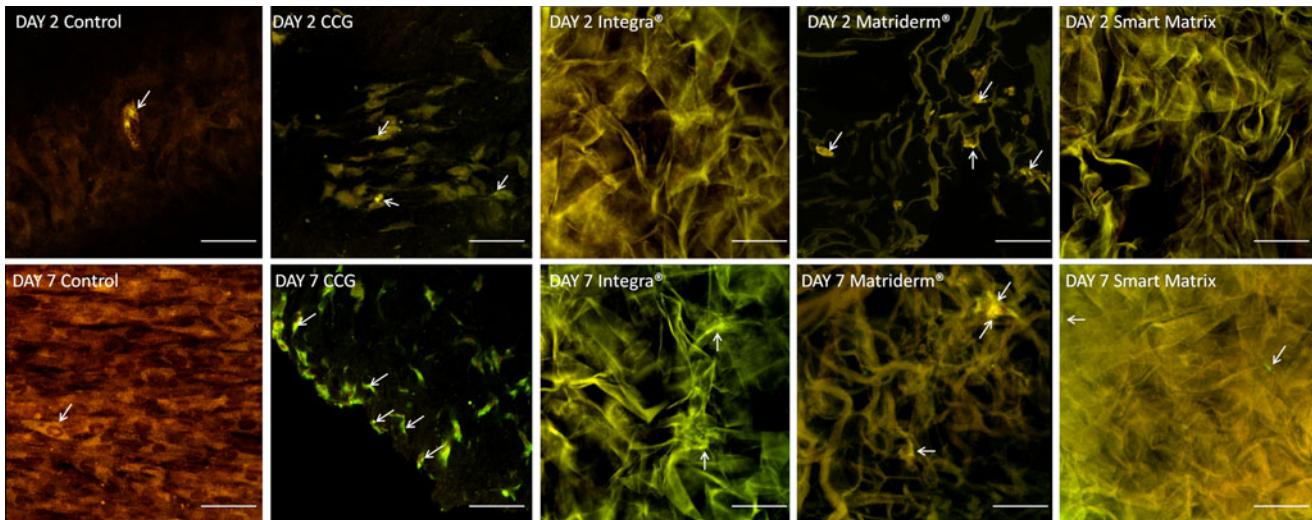


**FIG. 3.** Annexin V apoptosis assay. White arrows point at positively stained cells, which present an enhanced green fluorescence over background cells, stained in a green-yellow color. Scale bars = 50  $\mu$ m.

Moreover, at day 2, Smart Matrix was significantly higher than Matriderm ( $p=0.021$ ). Ki67 immunostaining, a cell proliferation marker, confirmed proliferation was maintained throughout the culture period.

#### Cell morphology

HDF monolayers under SEM showed a typical flattened, elongated morphology with multiple cytoplasmic processes of attachment to the surface and intercellular interactions (Fig. 2). In CCGs after 2 days of culture no surface cells were found, but after 7 days, cells with an irregular stellate shape were observed. The surfaces of dermal scaffolds at both time points were covered by a continuous layer of interconnected cells.

In histological cross-sections (Fig. 3), CCGs on day 2 showed either a rounded or stellate shape with long cytoplasmic processes, with markedly fewer ones by day 7. On dermal scaffold,

elongated cells were observed, which clearly predominated on Smart Matrix compared to Matriderm and Integra.

#### Annexin V apoptosis assay

Binding of annexin V protein to phosphatidylserine (PS) identifies PS flipping from the inner to the outlet layer of the cytoplasmic membrane, an early event in apoptosis.<sup>23</sup> Basal levels of apoptosis in proportion to cell density were seen in monolayer controls (Fig. 3).<sup>24</sup> Apoptosis markedly increased over the culture period for HDF cultured in CCGs,<sup>25</sup> and cells with disrupted morphology were clearly observed at day 7.

Apoptosis in Integra and Smart Matrix was partially masked by scaffold autofluorescence, although the apoptosis levels appeared to correlate with cell density. However, in Matriderm, apoptotic cells were clear, the level appearing higher at day 2 than day 7. These results corroborate the decreased activity observed in the alamarBlue assay for Matriderm at day 2.

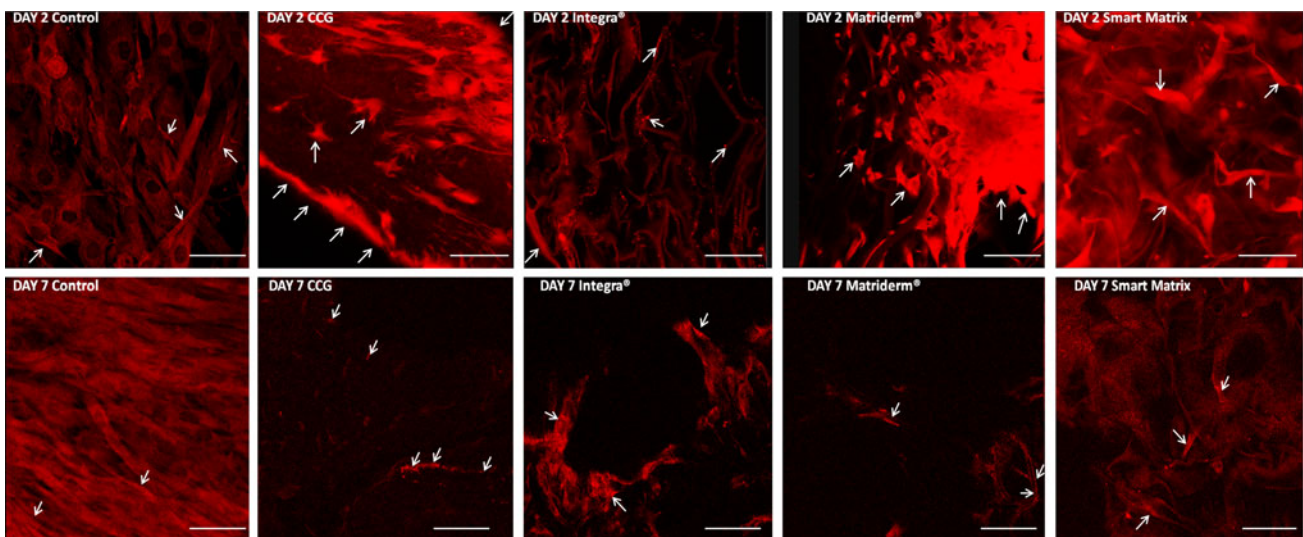


**FIG. 4.** Alpha-smooth muscle actin ( $\alpha$ -SMA) expression by immunostaining. White arrows point at positively stained cells, which present a bright red fluorescence. Scale bars = 50  $\mu$ m.

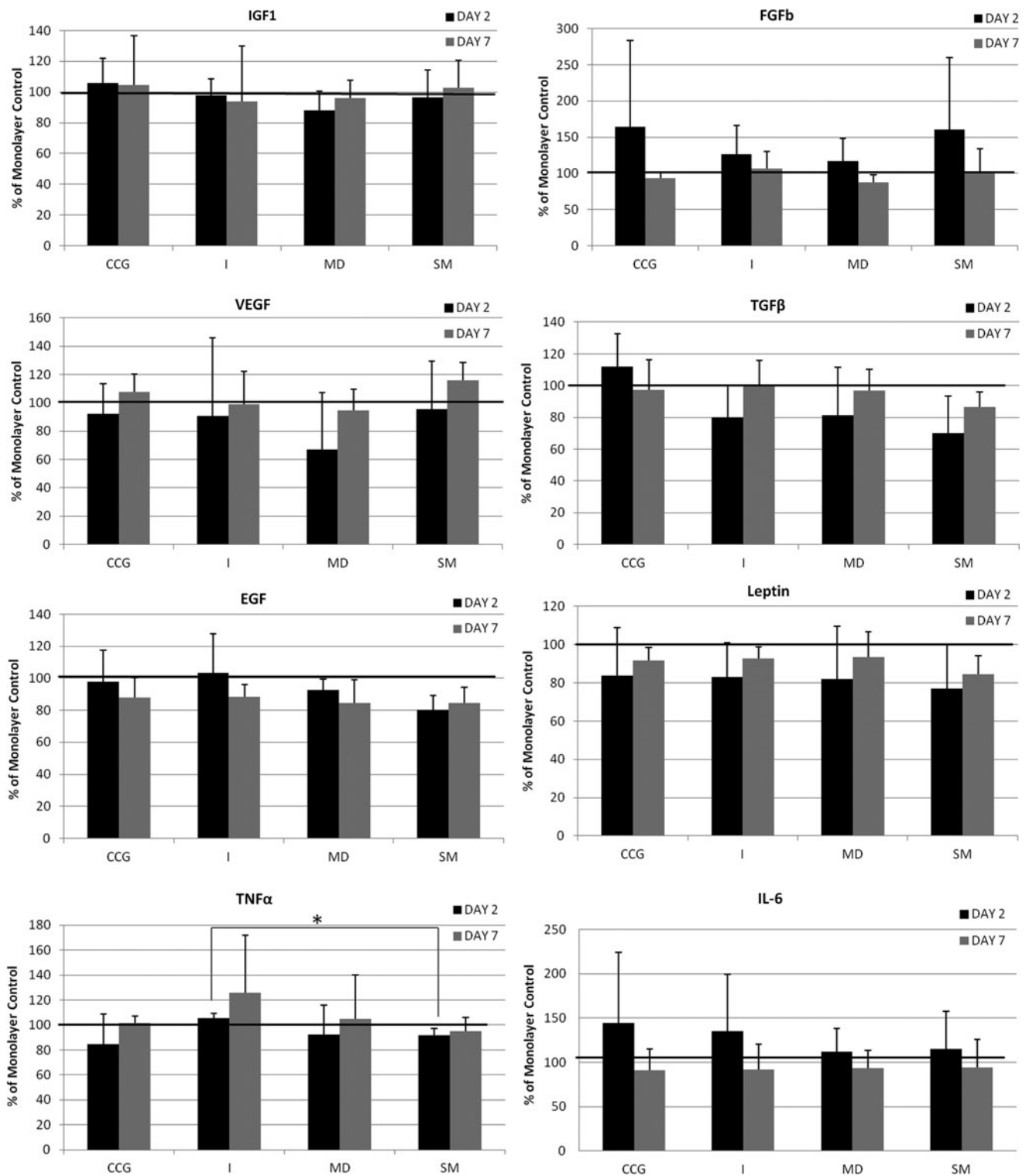


FIG. 5. Growth factor and cytokine expression profile of contractile collagen gels (CCG), Integra (I), Matriderm (MD), and Smart Matrix (SM) at days 2 and 7 of culture as percentage of monolayer control (\* $p=0.027$ ). TNF $\alpha$ , tumor necrosis factor alpha; IGF1, insulin-like growth factor 1; VEGF, vascular endothelial growth factor; IL, interleukin; bFGF, fibroblast growth factor b; TGF $\beta$ , transforming growth factor beta; EGF, epidermal growth factor.

TABLE 1. SCORING MATRIX

Parameter	Time point	Smart Matrix vs. CCG	Smart Matrix vs. Integra	Smart Matrix vs. Matriderm
Matrix contraction	2	1	0	0
	7	1	0	0
Cell viability + proliferation (alamarBlue assay)	2	0	0	1
	7	0	0	0
Cell viability + proliferation (Ki67 expression)	2	0	0	0
	7	0	0	0
Apoptosis (annexin V staining)	2	1	0	1
	7	1	0	0
Morphology (SEM)	2	1	0	0
	7	1	0	0
Morphology (H&E)	2	1	1	1
	7	1	1	1
$\alpha$ -SMA expression	2	1	0	1
	7	0	0	0
Cytokine and growth factor expression profile				
VEGF	2	0	0	0
	7	0	0	0
bFGF	2	0	0	0
	7	0	0	0
TGF $\beta$	2	0	0	0
	7	0	0	0
TNF $\alpha$	2	0	1	0
	7	0	0	0
IL-6	2	0	0	0
	7	0	0	0
IGF1	2	0	0	0
	7	0	0	0
Leptin	2	0	0	0
	7	0	0	0
EGF	2	0	0	0
	7	0	0	0
Total		9	3	5

CCG, contractile collagen gel; SEM, scanning electron microscopy; H&E, hematoxylin and eosin;  $\alpha$ -SMA, alpha-smooth muscle actin; VEGF, vascular endothelial growth factor; bFGF, fibroblast growth factor b; TGF $\beta$ , transforming growth factor beta; TNF $\alpha$ , tumor necrosis factor alpha; IL, interleukin; IGF1, insulin-like growth factor 1; EGF, epidermal growth factor.

#### $\alpha$ -SMA expression

$\alpha$ -SMA expression (Fig. 4) in monolayer controls was uniform across the sample, with some cells with dense  $\alpha$ -SMA filaments.<sup>26</sup> In CCGs,  $\alpha$ -SMA expression was greater towards the gel edge. Interestingly, in Integra at day 2,  $\alpha$ -SMA showed a speckled pattern but at day 7, bundles of  $\alpha$ -SMA filaments were apparent. In Matriderm,  $\alpha$ -SMA expression was intense and diffuse at day 2, and markedly decreased at day 7, with discrete filaments visible, associated with more elongated morphology. In Smart Matrix  $\alpha$ -SMA expression was relatively less intense and uniform at day 2, with positively stained filaments at day 7, concomitant with the elongated morphology.

#### Cytokine/growth factors expression profile

Expression of some factors (Fig. 5) was reduced in all matrices between day 2 and day 7 (bFGF, IL-6), whereas others increased (VEGF, leptin, TNF $\alpha$ ); for others, the effect varied with the matrix (EGF, TGF $\beta$ ). Expression of IGF1 was very similar to that of the monolayer control, and leptin levels in all 3D matrices were similarly lower than the monolayer controls. Of each scaffold, CCG gave highest bFGF, TGF $\beta$ , and IL-6 expression; Integra gave highest TNF $\alpha$  and high IL-6 expression;

Matriderm gave the lowest VEGF and bFGF expression and Smart Matrix gave highest VEGF, high bFGF, and lowest TGF $\beta$ , EGF, and TNF $\alpha$ . Only expression of TNF $\alpha$  at day 2 in Smart Matrix was significantly lower than in Integra ( $p=0.027$ ).

#### Scoring matrix

The scoring matrix (Table 1) showed that the new Smart Matrix had a positive total score over the three reference scaffolds.

#### Discussion

Classical *in vitro* testing of new dermal scaffolds includes cytotoxicity, mechanical characterization to exclude handling issues or poor mechanical stability, and investigation of certain cell–matrix interactions occurring during wound healing. However, an international standard *in vitro* model that studied the main events of wound healing and evaluated them in a combinatory manner by using a scoring matrix would predict *in vivo* outcomes such as integration, cellularization, and contraction of new dermal scaffolds and therefore would establish the necessity for further *in vivo* testing. The histological outcome of scaffold integration is shown by the

organization and morphology of fibroblasts, the major cell type in the dermis.<sup>10</sup> Their 3D ingress into dermal scaffolds *in vitro* was the basis for the described model.

The higher cell proliferation seen in Smart Matrix compared to Integra and Matriderm may be due to increased cell attachment, spreading, and infiltration,<sup>27</sup> suggesting that when implanted *in vivo* the influx of cells into Smart Matrix would be higher. A correlation between fibroblastoid morphology and phenotype has been long established. Fibroblasts present an elongated, spindle shape, while myofibroblasts, the contractile phenotype responsible for wound closure and scar contraction, show a flattened, irregular shape; the latter phenotype is associated with elevated  $\alpha$ -SMA expression.<sup>26,28</sup> This study demonstrates this correlation and suggests that cells keep the fibroblastic morphology when cultured on dermal scaffolds compared with CCGs. Moreover, Smart Matrix maintained the fibroblastic phenotype more efficiently than Integra or Matriderm, which could be predictive of reduced wound contraction and less scarring *in vivo*.

We found that the nature of the scaffold gives relatively subtle differences in the expression levels of several important factors, which may contribute to distinct outcomes. Only TNF $\alpha$  expression was significantly lower in Smart Matrix at day 2 compared to Integra. The pro-inflammatory cytokine TNF $\alpha$  may impair fibroblast ingress and promote myofibroblast differentiation through increasing the inflammatory component of the granulation response.<sup>29,30</sup> The significantly lower TNF $\alpha$  in Smart Matrix than in Integra at day 2 suggests a cellular response more supportive of fibroblast ingress in Smart Matrix.

The combinatorial evaluation of the results in the scoring matrix showed that Smart Matrix could offer an advantage over existing products and therefore should be further evaluated *in vivo*. Indeed, Smart Matrix has been shown to support rapid capillary formation and cellular ingress *in vivo*,<sup>31,32</sup> thus validating the proposed method, which would be useful as an international golden scoring matrix to develop new dermal scaffolds that effectively improve the existing products for better treatment of burns and chronic wounds.

### Acknowledgments

The authors express their gratitude to Zofia Luklinska (Nanovision Centre, Queen Mary's University of London) and Nimisha Patel (RAFT Institute of Plastic Surgery) for technical support.

### Author Disclosure Statement

No competing financial interests exist.

### References

- García-Gareta E, Ravindran N, Sharma V, Samizadeh S, Dye JF. A novel *in vitro* model of 3D cell ingress into scaffolds for dermal reconstruction to predict *in vivo* outcome. [Abstract.] TERMIS EU 2013 Annual Meeting, June 2013, Istanbul, Turkey. Abstract no. 665.
- García-Gareta E, Ravindran N, Sharma V, Samizadeh S, Dye JF. Prediction of *in vivo* outcome of new dermal scaffolds by a novel *in vitro* model of 3D cell ingress. [Abstract.] Tissue and Cell Engineering Society 2013 Annual Meeting, July 2013, Cardiff, United Kingdom. Eur Cell Mater. 2013;26 Suppl 7:55.
- García-Gareta E, Ravindran N, Sharma V, Samizadeh S, Dye JF. A novel multi-parameter *in vitro* model of 3D cell ingress into scaffolds for dermal reconstruction to predict *in vivo* outcome. [Abstract.] European Tissue Repair Society 2013 Annual Meeting, October 2013, Reims, France. Wound Repair Regen. 2013;21:A64.
- García-Gareta E, Ravindran N, Sharma V, Samizadeh S, Dye JF. A novel *in vitro* model of 3D cell ingress into scaffolds for dermal reconstruction to predict *in vivo* outcome. [Poster.] Available online at [www.raft.ac.uk/a-novel-in-vitro-model-of-3d-cell-ingress-into-scaffolds-for-dermal-reconstruction-to-predict-in-vivo-outcomes](http://www.raft.ac.uk/a-novel-in-vitro-model-of-3d-cell-ingress-into-scaffolds-for-dermal-reconstruction-to-predict-in-vivo-outcomes) (accessed October 23, 2013).
- Van der Veen VC, Van der Wal MBA, Van Leeuwen MCE, et al. Biological background of dermal substitutes. Burns. 2010;36:305–321.
- Dieckmann C, Renner R, Milkova L, et al. Regenerative medicine in dermatology: biomaterials, tissue engineering, stem cells, gene transfer and beyond. Experimental Dermatology. 2010;19:697–706.
- Auger FA, Berthod F, Moulin V, et al. Tissue-engineered skin substitutes: from *in vitro* constructs to *in vivo* applications. Biotechnol Appl Biochem. 2004;39:263–275.
- Dainiak MB, Allan IU, Savina IN, et al. Gelatin-fibrinogen cryogel dermal matrices for wound repair: preparation, optimisation and *in vitro* study. Biomaterials. 2010;31:67–76.
- Helary C, Bataille I, Abed A, et al. Concentrated collagen hydrogels as dermal substitutes. Biomaterials. 2010;31:481–490.
- Nolte SV, Xu W, Rennekampff HO, et al. Diversity of fibroblasts—a review on implications for skin tissue engineering. Cells Tissues Organs. 2008;187:165–176.
- Venugopal JR, Zhang Y, Ramakrishna S. *In vitro* culture of human dermal fibroblasts on electrospun polycaprolactone collagen nanofibrous membrane. Artif Organs. 2006;30:440–446.
- Ng KW, Tham W, Lim TC, et al. Assimilating cell sheets and hybrid scaffolds for dermal tissue engineering. J Biomed Mater Res. 2005;75A:425–438.
- Ojeh NO, Frame JD, Navsaria HA. *In vitro* characterization of an artificial dermal scaffold. Tissue Eng. 2001;7:457–472.
- Ma J, Wang H, He B, et al. A preliminary *in vitro* study on the fabrication and tissue engineering applications of a novel chitosan bilayer material as a scaffold of human neonatal dermal fibroblasts. Biomaterials. 2001;22:331–336.
- Bornstein MB. Reconstituted rattail collagen used as substrate for tissue cultures on coverslips in Maximow slides and roller tubes. Lab Invest. 1958;7:134–137.
- Linge C, Richardson J, Vigor C, et al. Hypertrophic scar cells fail to undergo a form of apoptosis specific to contractile collagen—the role of tissue transglutaminase. J Invest Dermatol. 2005;125:72–82.
- Frame JD, Still J, Lakhel-LeCoadou A, et al. Use of a dermal regeneration template in contracture release procedures: a multicenter evaluation. Plast Reconstr Surg. 2004;113:1330–1338.
- Jeng JC, Fidler PE, Sokolich JC, et al. Seven years' experience with Integra as a reconstructive tool. J Burn Care Res. 2007;28:120–126.
- Cuadra A, Correa G, Roa R, et al. Functional results of burned hands treated with Integra. J Plast Reconstr Aesthet Surg. 2012;65:228–234.
- Ryssel H, Gazyakan E, Germann G, et al. The use of Matriderm in early excision and simultaneous autologous skin grafting in burns—A pilot study. Burns. 2008;34:93–97.

21. Schneider J, Biedermann T, Widmer D, et al. Matriderm versus Integra: a comparative experimental study. *Burns*. 2009; 35:51–57.
22. Nociari MM, Shalev A, Benias P, et al. A novel one-step, highly sensitive fluorometric assay to evaluate cell-mediated cytotoxicity. *J Immunol Methods*. 1998;213:157–167.
23. Alberts B, Johnson A, Lewis J, et al. *Molecular Biology of the Cell, 5th edition*. Oxford: Garland Science, 2008.
24. Mammine T, Gan D, Foyouzi-Youssefi R. Apoptotic cell death increases with senescence in normal human dermal fibroblasts cultures. *Cell Biol Int*. 2006;30:903–909.
25. Fluck J, Querfeld C, Cremer A, et al. Normal human primary fibroblasts undergo apoptosis in three-dimensional contractile collagen gels. *J Invest Dermatol*. 1998;110: 153–157.
26. Matthey DL, Dawes PT, Nixon NB, Slater H. Transforming growth factor  $\beta$ 1 and interleukin 4 induced  $\alpha$  smooth muscle actin expression and myofibroblasts-like differentiation in human synovial fibroblasts in vitro: modulation by basic fibroblast growth factor. *Ann Rheum Dis*. 1997;56: 426–431.
27. Ahmed TAE, Dare EV, Hincke M. Fibrin: a versatile scaffold for tissue engineering applications. *Tissue Eng Part B*. 2008; 14:199–215.
28. Hinz B, Mastrangelo D, Iselin CE, et al. Mechanical tension controls granulation tissue contractile activity and myofibroblasts differentiation. *Am J Pathol*. 2001;159: 1009–1020.
29. Barrientos S, Stojadinovic O, Golinko MS, et al. Growth factors and cytokines in wound healing. *Wound Rep Reg*. 2008;16:585–601.
30. Werner S, Grose R. Regulation of wound healing by growth factors and cytokines. *Physiol Rev*. 2003;83:835–870.
31. Taheri A, Patel N, Dann SC, Dye JF. Vasculogenesis in rapid integration of a synthetic dermal scaffold: efficacy for single-stage full thickness surgical reconstruction. *TERMIS EU Galway*. 2010. Abstract 339.
32. Dye JF, Dann SC, Baldwin C. Intersecting design criteria for development of a “Smart Matrix” synthetic dermal replacement. *TERMIS EU Galway*. 2010. Abstract 356.

Address correspondence to:  
 Elena García-Gareta, PhD, MSc  
 RAFT Institute of Plastic Surgery  
 Leopold Muller Building  
 Mount Vernon Hospital  
 Northwood HA6 2RN  
 United Kingdom

E-mail: garciae@raft.ac.uk

#### Abbreviations Used

3D = three-dimensional  
 $\alpha$ -SMA = alpha-smooth muscle actin  
 bFGF = fibroblast growth factor b  
 BSA = bovine serum albumin  
 CCG = contractile collagen gel  
 DMEM = Dulbecco's modified Eagle's medium  
 EGF = epidermal growth factor  
 HDF = human dermal fibroblast  
 IGF1 = insulin-like growth factor 1  
 IL = interleukin  
 PBS = phosphate-buffered saline  
 PS = phosphatidylserine  
 SEM = scanning electron microscopy  
 TGF $\beta$  = transforming growth factor beta  
 TNF $\alpha$  = tumor necrosis factor alpha  
 VEGF = vascular endothelial growth factor